NANO LETTERS
Letter
Cite This: Nano Lett. 2018, 18, 2525−2529
pubs.acs.org/NanoLett

The Interfacial Assembly of Polyoxometalate Nanoparticle Surfactants

Caili Huang,[†,∥] Yu Chai,[‡] Yufeng Jiang,[§] Joe Forth,[§] Paul D. Ashby,[‡] Matthias M. L. Arras,[∥] Kunlun Hong,[⊥] Gregory S. Smith,[∥] Panchao Yin,*[,#] and Thomas P. Russell*[,†,§,▽]

[†]Polymer Science and Engineering Department, University of Massachusetts, 120 Governors Drive, Conte Center for Polymer Research, Amherst, Massachusetts 01003, United States

[‡]The Molecular Foundry and [§]Materials Sciences Divsion, Lawrence Berkeley National Laboratory, One Cyclotron Road, Berkeley, California 94720, United States

[∥]Neutron Scattering Division and [⊥]Center for Nanophase Materials Sciences, Oak Ridge National Laboratory, Oak Ridge, Tennessee 37831, United States

[#]South China Advanced Institute for Soft Matter Science and Technology, South China University of Technology, Guangzhou 510640, China

[▽]Beijing Advanced Innovation Center for Soft Matter Science and Engineering, Beijing University of Chemical Technology, Beijing 100029, China

Supporting Information

ABSTRACT: Polyoxometalates (POMs) using $\{Mo_{72}V_{30}\}$ as an example, dissolved in water, can interact with amine-terminated polydimethylsiloxane (PDMS-NH_2) dissolved in toluene at the water/toluene interface to form POM-surfactants that significantly lower the interfacial tension and can be used to stabilize liquids via interfacial elasticity. The jamming of the POM-surfactants at the water/oil interface with consequent wrinkling occurs with a decrease in the interfacial area. The packing density of the POM-surfactants at the interface can be tuned by varying the strength of screening with the addition of cations with differing hydrated radii.

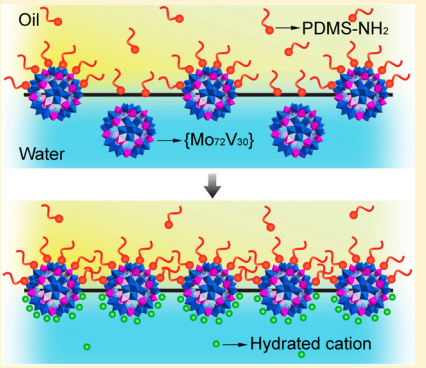

KEYWORDS: *POM-surfactant, liquid/liquid interfaces, structured liquids, self-assembly, wrinkling*

Colloidal particles can assemble at oil−water interfaces, screening energetically costly interfacial interactions between immiscible liquids.[1−5] Particles that are strongly bound to the interface can impart mechanical integrity to the assembly. These quasi-two-dimensional assemblies can support anisotropic stresses, giving rise to a wealth of complex, non-equilibrium, all liquid structures.[3,6,7] The energy binding particles to the interface increases quadratically with particle radius,[3] and so in the case of nanoparticles (NPs) the reduction in the interfacial energy per NP is small. Therefore, compressive forces exerted on the NPs as the interfacial area decreases are sufficient to eject the NPs from the interface, causing the liquid/liquid interface to ultimately relax to an equilibrium spherical shape. As such, it is difficult to structure liquids into nonequilibrium shapes with uniformly functionalized NPs. Janus-type NPs can be prepared where the reduction in the interfacial energy per NP is greater but, as of yet, they have not been used to structure liquids into complex shapes.[8,9] Janus-type polymeric particles, specifically Janus-star shaped copolymers, as described by Müller and co-workers[10,11] and by Jiang et al.[12] can be used to shape liquids; however, the polymer chains can contract upon compression and the loading of the star-shaped polymers at the interface must be exceptionally high to effect tailored shaping of the liquids. Recently, a very simple method was developed where NP-surfactants were formed at liquid/liquid interfaces by dispersing functionalized NPs in one fluid and polymers end-capped with a complementary functionality in an immiscible second fluid.[13] The NPs and polymers will interact at the interface, forming NP-surfactants having hydrophilic NP heads anchored by hydrophobic polymer tails. The NP-surfactants assemble spontaneously into a monolayer at the interface and the assemblies self-regulate by tuning the numbers of polymer chains interacting with the NPs. This strategy not only circumvents the detailed chemistries necessary to precisely functionalize the NPs but also affords a simple pathway to structure the liquids into highly nonequilibrium

Received: January 16, 2018
Revised: February 9, 2018
Published: March 20, 2018

DOI: 10.1021/acs.nanolett.8b00208
Nano Lett. 2018, 18, 2525−2529

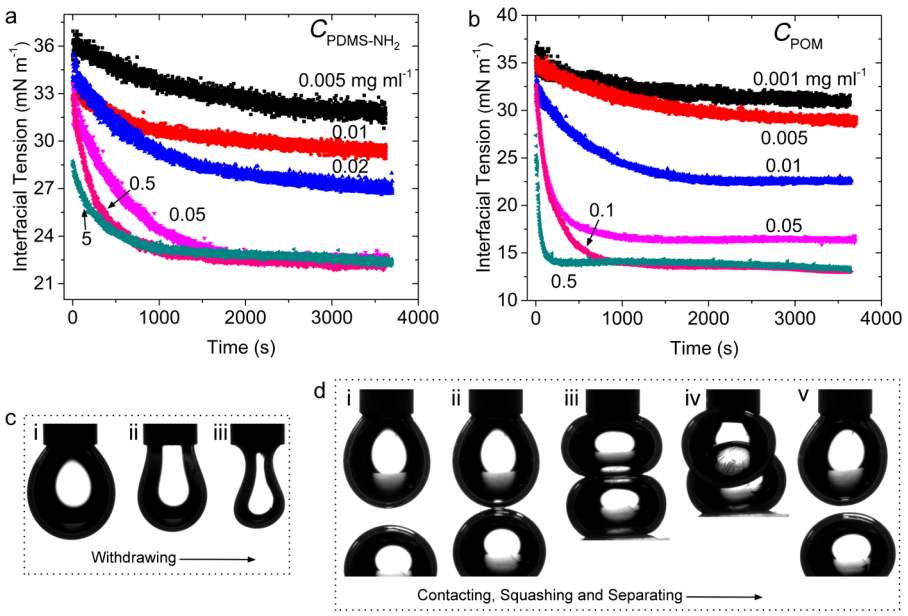

Figure 1. (a) Dynamic interfacial tension of 0.01 mg mL^{-1} $\{Mo_{72}V_{30}\}$ aqueous solution in contact with a toluene solution of PDMS-NH_2 at different concentrations. (b) Dynamic interfacial tension for a fixed concentration of PDMS-NH_2 (0.05 mg mL^{-1}) with an increasing concentration of the $\{Mo_{72}V_{30}\}$ from 0.001 to 0.5 mg mL^{-1}. (c) Droplet morphology and its buckling behavior when $\{Mo_{72}V_{30}\}$ aqueous solution was withdrawn. Droplet was formed by injecting 0.5 mg mL^{-1} $\{Mo_{72}V_{30}\}$ aqueous solution into 0.05 mg mL^{-1} PDMS-NH_2 toluene solution. (d) Sequence of snapshots showing the process of contact, compression, and separation of two droplets. Droplets were formed by injecting 0.5 mg mL^{-1} $\{Mo_{72}V_{30}\}$ aqueous solution into 5 mg mL^{-1} PDMS-NH_2 toluene solution and the bottom droplet was formed prior to the experiment and rested at the bottom of the cuvette. Note that, after compression and expansion the droplet shape has changed due to the plastic deformation of the POM-surfactant assembly.

shapes,[13] including bicontinuous interfacially jammed emulsion gels, called "bijels".[14] In situ NP-surfactant formation opens a new concept for material design, and the ability to generate all-liquid bijels with bicontinuous fluid channels enables the continuous cross-transport or cross-flow of fluids with potential applications as multiphase microreactors, microfluidic devices, all-liquid membranes, and multilength scale porous materials.[15−18] Furthermore, the bonding between the NPs and end-functionalized polymers that result in the formation of the NP-surfactants is not covalent and the resultant assemblies are jammed; consequently, the NP-surfactant assemblies are responsive to external stimuli and the systems are reconfigurable.[19]

Polyoxometalates (POMs), well-defined molecular clusters comprised of early transition metal ions and oxo ligands having sizes ranging from 1 to 6 nm, provide an interesting candidate for use as NPs in the formation of NP-surfactants.[20−22] The inorganic chemistries associated with POMs have been extensively studied, including their synthesis, catalytic, and self-assembly behavior in water.[22−26] In comparison to classic NPs, POMs are monodisperse, have well-defined structures, and have tunable surface properties, such as charge density.[22] Diverse applications have emerged for POMs, for example as building blocks in supramolecular chemistry and as physical models for nanoconfinement effects and the polyelectrolytes.[21,22,27−29] POM−organic hybrids have been used as emulsion catalysts to bridge the reactions between immiscible phases.[30−34] To mimic the functions of cell membranes with POM materials, inorganic chemical cells can be obtained at the diffusive layers between aqueous solutions of POMs and large cations.[35] Taking advantage of supramolecular interactions between POMs and polymers (for example, electrostatic attraction), POM-based nanocomposites with controllable morphology and order-structure were prepared.[36−38] However, little attention has been given to the interfacial activity of POMs between two immiscible liquids nor to their use to structure the liquids.

Here, we present a study on the formation and assembly of the POM-surfactants at liquid/liquid interfaces and highlight the tunable packing behavior of POM-surfactant assemblies. $\{Mo_{72}V_{30}\}$,[39,40] a typical 2.5 nm Keplerate molecular cluster, comprised of 12 pentagonal $\{(Mo^{VI})Mo^{VI}_5\}$ units connected by 30 V^{IV} linkers with a hollow spherical structure, was used in this study. Its crystalline molecular formula is $Na_8K_{14}(VO)_2[\{(Mo)Mo_5O_{21}(H_2O)_3\}_{10}\{(Mo)Mo_5O_{21}(H_2O)_3(SO_4)\}_2\{VO(H_2O)\}_{20}\{VO\}_{10}(\{KSO_4\}_5)_2]\cdot 150H_2O$ (molecular weight = 19048 g mol^{-1}), and the molecular formula after dissolving in water usually represents as $[Mo_{72}V_{30}O_{320}S_{12}]^{31-}$. $\{Mo_{72}V_{30}\}$ is stable when dissolved in water and is a discrete macroanion that carries 31 negative charges on the surface (balanced by countercations). $\{Mo_{72}V_{30}\}$ is not active at the toluene/water interface (Figure S1), where the interfacial tension (γ) between water and toluene is ∼34.5 mN m^{-1}, very close to the textbook values for γ between pure water and toluene of 36 mN m^{-1}. Amine-terminated polydimethylsiloxane, PDMS-NH_2, dissolved in toluene on the other hand, does act as surfactant at the toluene/water interface, reducing the γ to 26 mN m^{-1} at a PDMS-NH_2 concentration of 5 mg mL^{-1} (Figure S1). With the addition of $\{Mo_{72}V_{30}\}$ (0.01 mg mL^{-1}, ∼5.2 × 10^{-7} mmol ml^{-1}) to the aqueous phase (Figure 1a), γ further decreases to 22 mN m^{-1} during the same period (usually measured after 1 h), demonstrating a significant reduction in interfacial energy associated with POM-surfactant formation and assembly at the interface. The negatively charged $\{Mo_{72}V_{30}\}$ and protonated PDMS-NH_2, that is, PDMS-NH_3^+, where the pH of $\{Mo_{72}V_{30}\}$ aqueous is ∼3.9 and the pK_a of −NH_2 is ∼9[19], give rise to strong electrostatic interactions and binding of the two at the interface. As a result, a POM-surfactant monolayer assembly

DOI: 10.1021/acs.nanolett.8b00208
Nano Lett. 2018, 18, 2525−2529

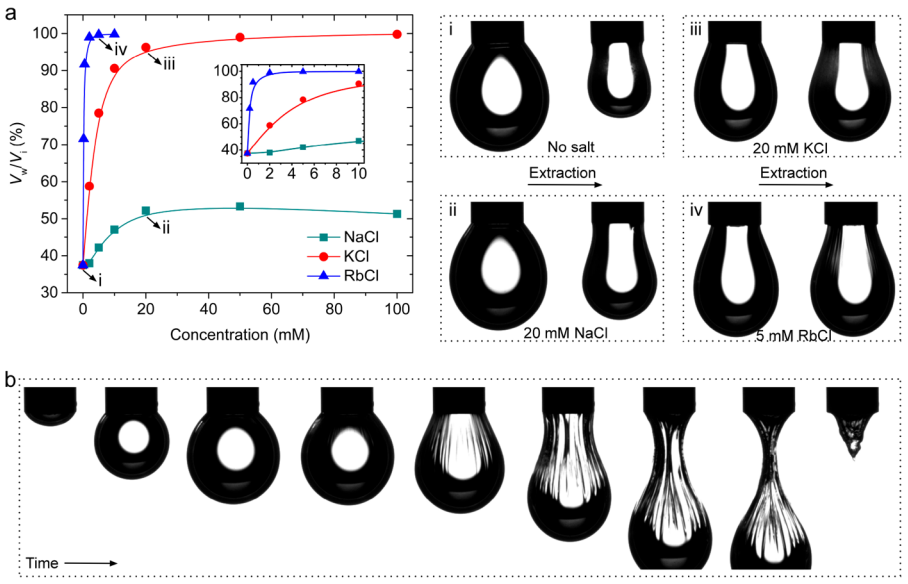

Figure 2. (a) Compression ratio of aged droplets of water with 0.2 mg mL^{-1} $\{Mo_{72}V_{30}\}$ immersed in toluene with 0.05 mg mL^{-1} PDMS-NH_2 measured by withdrawing the aqueous solution from pendent drop after 1 h of aging at different NaCl, KCl, and RbCl concentrations and snapshots of the droplets during the withdrawal process at 0 and 20 mM NaCl, 20 mM KCl, and 5 mM RbCl, respectively. (b) A series of snapshots showing the evolution of a droplet that was injected from 0.2 mg mL^{-1} $\{Mo_{72}V_{30}\}$ aqueous solution with 10 mM RbCl into a 0.05 mg mL^{-1} PDMS-NH_2 toluene solution.

forms at the interface. In a typical POM-surfactant system, when the concentrations of the PDMS-NH_2 solutions are varied and the aqueous solution of $\{Mo_{72}V_{30}\}$ is fixed at 0.01 mg mL^{-1}, γ is found to decrease with increasing PDMS-NH_2 concentration. Above a concentration of 0.05 mg mL^{-1}, γ did not decrease further and remained constant at ~22 mN m^{-1}. Here, the rate of reduction in γ increased with increasing PDMS-NH_2 concentration. In all instances, after the initial reduction in γ, there is a second slower process that leads to a continued slight decrease in γ with time. We attribute this slow process to the rearrangement of the POM-surfactant monolayer at the interface.

On the other hand, if the concentration of PDMS-NH_2 was fixed at 0.05 mg mL^{-1} and the concentration of $\{Mo_{72}V_{30}\}$ varied, the results in Figure 1b were obtained. For lower concentration of $\{Mo_{72}V_{30}\}$ (<0.01 mg mL^{-1}), the reduction in γ is gradual. This is a result of the diffusion of POMs to the interface, the formation of POM-surfactants at the interface, and the reorganization necessary for subsequent POMs to be anchored to the interface. However, as the concentration of POMs is increased, the reduction in γ is much more rapid, and the equilibrium in γ is much lower ~13 mN m^{-1}. Consequently, upon decreasing the volume of the droplet the POM-surfactant assemblies wrinkle, which is characteristic of a jammed assembly (Figure 1c and Movie S1). The droplets do not coalesce even when forced into contact (Figure 1d and Movie S2). During the compression, as the droplet's interfacial area is reduced, the POM-surfactant assemblies jam causing either a wrinkling of the assembly or a permanent distortion of the droplet shape when the droplets are separated.

The variation in the packing density of the POM-surfactants was investigated by the addition of salt to the aqueous phase to tune the surface properties of $\{Mo_{72}V_{30}\}$. When the volume of the droplet coated with the POM-surfactants is decreased to the point where wrinkling occurs, this onset-of-wrinkling volume can be used as a measure of the initial packing density of the POM-surfactants at the interface; V_w/V_i is the amount that the initial assembly of the POM-surfactants must be compressed to solidify the assemblies, wheres V_w is the volume of the droplet when wrinkling is observed and V_i is the initial volume of a droplet. Figure 2a shows the value of V_w/V_i as a function of concentration of different salts after aging for 1 h. The snapshots were captured when the aqueous phase was withdrawn from the droplets. For each of the snapshots, the image was on the left-hand side (lhs) taken after 1 h aging, whereas the image on the right-hand side (rhs) shows the initial visible wrinkling state (Figure 2a and Movie S3–S6). It is evident that V_w/V_i depends on the type of salt added to the aqueous phase. Without the salt, V_w/V_i was ~0.37, whereas it gradually increased to ~0.52 with increasing concentration of NaCl. This saturates at a NaCl concentration of 20 mM. These results show that NaCl promotes the assembly of POM-surfactants at the interface. On the other hand, adding KCl or RbCl to the aqueous phase leads to much higher initial packing density of POM-surfactants. V_w/V_i rapidly increased to near unity, especially for the RbCl, V_w/V_i increased to 0.98 with the addition of only 2 mM salt, indicating a near complete coverage of the interface with POM-surfactants initially. When the concentration of RbCl is increased to 10 mM, the droplet self-wrinkles after ~55 s, as shown in the third to fourth images in Figure 2b. The self-wrinkled droplet eventually fell from the needle (Figure 2b and Movie S7). This self-wrinkling behavior demonstrates the ability of the salt to promote the formation and assembly of the POM-surfactants, the significant reduction in the interfacial tension (Figure S4 and S5) that allows the droplet shape to extend (significantly increasing the interfacial area), and the budding-off of the droplet. Gravitational forces underpin the extension of the droplet.

$\{Mo_{72}V_{30}\}$ carries 31 negative charges on its surface, theoretically balanced by 8 Na^+, 14 K^+, 2 VO^{2+}, and 5 H_3O^+ counter-cations. A very interesting and reasonable explanation for the above results is that the affinity of cations to the $\{Mo_{72}V_{30}\}$ macroions relies on the size of hydrated cations. The smaller the size of the hydrated cations, the stronger of the affinity. Here, we chose the monovalent cations Na^+, K^+, and Rb^+, thus

DOI: 10.1021/acs.nanolett.8b00208
Nano Lett. 2018, 18, 2525–2529

the ionic strength is the same at a fixed concentration. Rb^+ has the smallest hydrated size such that it can replace the original countercations with a stronger affinity to the $\{Mo_{72}V_{30}\}$ macroions.[39] This stronger affinity reduces the repulsion between the $\{Mo_{72}V_{30}\}$ macroions, promoting the formation of POM-surfactants and the generation of high areal density POM-surfactant assemblies at the interface. This is essentially a screening effect (Figure 3). Na^+, however, is less likely to

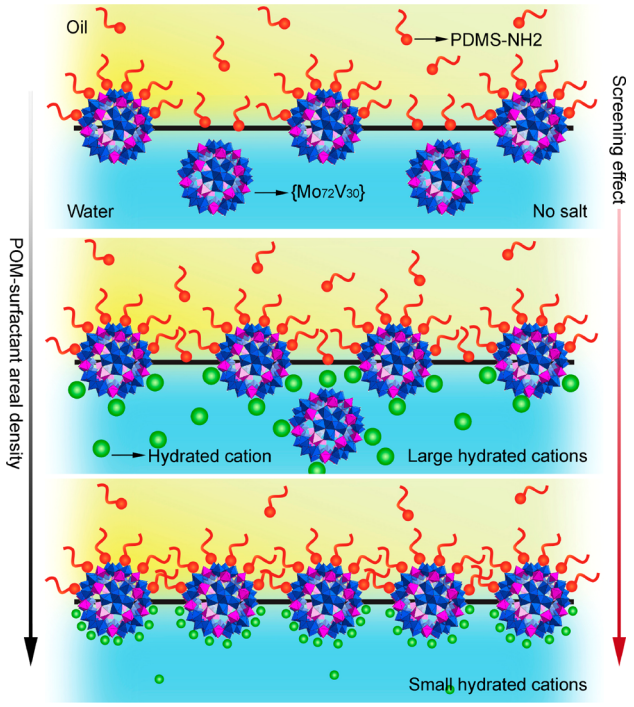

Figure 3. Schematic diagram of the POM-surfactants assembled at the water/toluene interface at different screening effect conditions.

exchange with the countercations, resulting in a smaller increase in the packing density of POM-surfactants at the interface. The observed self-wrinkling, extension and breaking off of the droplet (Figure 2b), can be attributed to the high packing density of the POM-surfactants, including the counter Rb^+ and the continuous decrease in γ with time (Figure S4, even though the initial γ is not that low, Figure S5). If more RbCl, for example, 20 mM, was added to the aqueous phase, the $\{Mo_{72}V_{30}\}$ precipitated due to the excess screening effects (Figure S7), which is evidenced by the lack of wrinkling after aging 1 h.

We have demonstrated the interfacial activity of $\{Mo_{72}V_{30}\}$ to interact with PMDS-NH_2 at a water/toluene interface to form POM-surfactants that considerably reduce interfacial tension. The jamming and wrinkling of the interfacial POM-surfactant assemblies were observed when the interfacial area was decreased. The packing density of $\{Mo_{72}V_{30}\}$ at the water/toluene interface was tuned by adding different salts where the size of the hydrated cations appeared to be of importance, with the screening of repulsive interaction between the POMs promoted a denser packing of the POM-surfactants at the interface.

■ ASSOCIATED CONTENT

Supporting Information

The Supporting Information is available free of charge on the ACS Publications website at DOI: 10.1021/acs.nanolett.8b00208.

Materials and methods, γ of water/toluene and POM-surfactant monolayer assembly (Figure S1−S6), the DLS data of POM aqueous (Figure S7) (PDF)
Movie S1 of droplet (AVI)
Movie S2 of droplet (AVI)
Movie S3 of droplet (AVI)
Movie S4 of droplet (AVI)
Movie S5 of droplet (AVI)
Movie S6 of droplet (AVI)
Movie S7 of droplet (AVI)

■ AUTHOR INFORMATION

Corresponding Authors

*E-mail: yinpc@scut.edu.cn.
*E-mail: russell@mail.pse.umass.edu.

ORCID

Caili Huang: 0000-0003-1209-1141
Paul D. Ashby: 0000-0003-4195-310X
Matthias M. L. Arras: 0000-0002-4714-9086
Kunlun Hong: 0000-0002-2852-5111
Panchao Yin: 0000-0003-2902-8376
Thomas P. Russell: 0000-0001-6384-5826

Notes

The authors declare no competing financial interest.

■ ACKNOWLEDGMENTS

This work was supported by the U.S. Department of Energy, Office of Science, Basic Energy Sciences, Materials Sciences and Engineering Division under Award under Contract No. DE-CA02-05-CH11231 within the Adaptive Interfacial Assemblies Towards Structuring Liquids program (KCTR16). The research at Oak Ridge National Laboratory was sponsored by the Scientific User Facilities Division, Office of Basic Energy Sciences, U.S. Department of Energy.

■ REFERENCES

(1) Pickering, S. U. *J. Chem. Soc., Trans.* **1907**, *91*, 2001−2021.
(2) Pieranski, P. *Phys. Rev. Lett.* **1980**, *45*, 569−572.
(3) Lin, Y.; Skaff, H.; Emrick, T.; Dinsmore, A. D.; Russell, T. P. *Science* **2003**, *299*, 226−229.
(4) Zhang, J.; Coulston, R. J.; Jones, S. T.; Geng, J.; Scherman, O. A.; Abell, C. *Science* **2012**, *335*, 690−694.
(5) Binks, B. P. *Curr. Opin. Colloid Interface Sci.* **2002**, *7*, 21−41.
(6) Stratford, K.; Adhikari, R.; Pagonabarraga, I.; Desplat, J. C.; Cates, M. E. *Science* **2005**, *309*, 2198−2201.
(7) Lin, Y.; Skaff, H.; Böker, A.; Dinsmore, A. D.; Emrick, T.; Russell, T. P. *J. Am. Chem. Soc.* **2003**, *125*, 12690−12691.
(8) Chen, Q.; Whitmer, J. K.; Jiang, S.; Bae, S. C.; Luijten, E.; Granick, S. *Science* **2011**, *331*, 199−202.
(9) Chen, Q.; Bae, S. C.; Granick, S. *J. Am. Chem. Soc.* **2012**, *134*, 11080−11083.
(10) Hanisch, A.; Gröschel, A. H.; Förtsch, M.; Drechsler, M.; Jinnai, H.; Ruhland, T. M.; Schacher, F. H.; Müller, A. H. E. *ACS Nano* **2013**, *7*, 4030−4041.
(11) Ruhland, T. M.; Gröschel, A. H.; Walther, A.; Müller, A. H. E. *Langmuir* **2011**, *27*, 9807−9814.
(12) Jiang, Y.; Löbling, T. I.; Huang, C.; Sun, Z.; Müller, A. H. E.; Russell, T. P. *ACS Appl. Mater. Interfaces* **2017**, *9*, 33327−33332.
(13) Cui, M.; Emrick, T.; Russell, T. P. *Science* **2013**, *342*, 460−463.
(14) Huang, C.; Forth, J.; Wang, W.; Hong, K.; Smith, G. S.; Helms, B. A.; Russell, T. P. *Nat. Nanotechnol.* **2017**, *12*, 1060−1063.
(15) Herzig, E. M.; White, K. A.; Schofield, A. B.; Poon, W. C. K.; Clegg, P. S. *Nat. Mater.* **2007**, *6*, 966−971.
(16) Lee, M. N.; Mohraz, A. *Adv. Mater.* **2010**, *22*, 4836−4841.

DOI: 10.1021/acs.nanolett.8b00208
Nano Lett. 2018, 18, 2525−2529

(17) Lee, M. N.; Mohraz, A. *J. Am. Chem. Soc.* **2011**, *133*, 6945−6947.
(18) Haase, M. F.; Stebe, K. J.; Lee, D. *Adv. Mater.* **2015**, *27*, 7065−7071.
(19) Huang, C.; Sun, Z.; Cui, M.; Liu, F.; Helms, B. A.; Russell, T. P. *Adv. Mater.* **2016**, *28*, 6612−6618.
(20) Müller, A.; Roy, S. *Coord. Chem. Rev.* **2003**, *245*, 153−166.
(21) Müller, A.; Gouzerh, P. *Chem. Soc. Rev.* **2012**, *41*, 7431−7463.
(22) Yin, P.; Li, D.; Liu, T. *Chem. Soc. Rev.* **2012**, *41*, 7368−7383.
(23) Cronin, L.; Müller, A. *Chem. Soc. Rev.* **2012**, *41*, 7333−7334.
(24) Wang, S.-S.; Yang, G.-Y. *Chem. Rev.* **2015**, *115*, 4893−4962.
(25) Carr, R.; Weinstock, I. A.; Sivaprasadarao, A.; Müller, A.; Aksimentiev, A. *Nano Lett.* **2008**, *8*, 3916−3921.
(26) Bodnarchuk, M. I.; Erni, R.; Krumeich, F.; Kovalenko, M. V. *Nano Lett.* **2013**, *13*, 1699−1705.
(27) Baruah, B.; Swafford, L. A.; Crans, D. C.; Levinger, N. E. *J. Phys. Chem. B* **2008**, *112*, 10158−10164.
(28) Long, D.-L.; Tsunashima, R.; Cronin, L. *Angew. Chem., Int. Ed.* **2010**, *49*, 1736−1758.
(29) Bera, M. K.; Ellis, R. J.; Burton-Pye, B. P.; Antonio, M. R. *Phys. Chem. Chem. Phys.* **2014**, *16*, 22566−22574.
(30) Li, B.; Li, W.; Li, H.; Wu, L. *Acc. Chem. Res.* **2017**, *50*, 1391−1399.
(31) Yin, P.; Wang, J.; Xiao, Z.; Wu, P.; Wei, Y.; Liu, T. *Chem. - Eur. J.* **2012**, *18*, 9174−9178.
(32) Leclercq, L.; Mouret, A.; Proust, A.; Schmitt, V.; Bauduin, P.; Aubry, J.-M.; Nardello-Rataj, V. *Chem. - Eur. J.* **2012**, *18*, 14352−14358.
(33) Leclercq, L.; Mouret, A.; Bauduin, P.; Nardello-Rataj, V. *Langmuir* **2014**, *30*, 5386−5393.
(34) Kida, T.; Matsufuji, H.; Yuasa, M.; Shimanoe, K. *Langmuir* **2013**, *29*, 2128−2135.
(35) Cooper, G. J. T.; Kitson, P. J.; Winter, R.; Zagnoni, M.; Long, D.-L.; Cronin, L. *Angew. Chem., Int. Ed.* **2011**, *50*, 10373−10376.
(36) Bu, W.; Uchida, S.; Mizuno, N. *Angew. Chem., Int. Ed.* **2009**, *48*, 8281−8284.
(37) Lunkenbein, T.; Kamperman, M.; Li, Z.; Bojer, C.; Drechsler, M.; Förster, S.; Wiesner, U.; Müller, A. H. E.; Breu, J. *J. Am. Chem. Soc.* **2012**, *134*, 12685−12692.
(38) Zhang, Q.; Liao, Y.; He, L.; Bu, W. *Langmuir* **2013**, *29*, 4181−4186.
(39) Pigga, J. M.; Kistler, M. L.; Shew, C.-Y.; Antonio, M. R.; Liu, T. *Angew. Chem., Int. Ed.* **2009**, *48*, 6538−6542.
(40) Müller, A.; Todea, A. M.; van Slageren, J.; Dressel, M.; Bögge, H.; Schmidtmann, M.; Luban, M.; Engelhardt, L.; Rusu, M. *Angew. Chem., Int. Ed.* **2005**, *44*, 3857−3861.

DOI: 10.1021/acs.nanolett.8b00208
Nano Lett. 2018, 18, 2525−2529